KI-67 AND MICRORNA-27A IN THE LESION TISSUES OF PATIENTS WITH EARLY GASTRIC CANCER AND THEIR CORRELATION WITH THE DEPTH OF INFILTRATION

Minxia Qiu, Cancan Kong, Wenmei Chen, Wei Mao*
Endoscopic diagnosis and treatment center, Hainan Provincial People's Hospital, Haikou 570311, Hainan Province, China

ABSTRACT

This study aimed to explore the roles and molecular mechanisms of Ki-67 and microRNA-27a (miR-27a) in organ-specific gastric cancer (GC) metastasis to further clarify the mechanism of GC metastasis and provide a theoretical basis for identifying new therapeutic targets of advanced GC. We collected and processed GC samples, which then underwent microRNA extraction and immunohistochemical staining. Following the assessment of Ki-67 and miR-27a expression in GC tissues and normal gastric mucosa samples, we analyzed the relationships between Ki-67 and miR-27a expression in GC patients and gender, age, tumor location, size, general type, differentiation degree, invasion depth, lymph node metastasis, clinical department, as well as the relationship between clinical and biological behaviors. Ki-67 positive signals were primarily expressed in the nuclei of normal gastric tissue. Among 10 normal gastric tissues, 5 were Ki-67 negative, 4 were weakly positive, 1 was moderately positive, and 0 were strongly positive. In 80 GC tissues, 24 were Ki-67 negative, 12 were weakly positive, 18 were moderately positive, and 26 were strongly positive. Ki-67 expression increased gradually with the increase of tumor focus, differentiation degree, invasion depth, lymph node metastasis, clinical division, and the malignant degree of GC. It demonstrated a higher and faster growth rate and gradually increased aggression and transferability.

Keywords: *Ki-67, microRNA-27a, gastric cancer patients, depth of infiltration.*

DOI: 10.19193/0393-6384_2023_4_146

Received *January 15, 2023;* ***Accepted*** *April 20, 2023*

Introduction

In recent years, there has been significant development in modern medical science and technology, such as in molecular biology, molecular immunology, and molecular genetics[1-2]. The development of gastric cancer (GC) results from the accumulation of various genetic changes and is caused by the activation of several original cancer genes and the inactivation of several anti-cancer genes[3]. Tumor cells have specific metastasis-related molecules. Identifying specific molecules for GC metastasis, particularly liver metastasis, can improve diagnosis efficacy[4-5]. In recent years, research on tumor markers has achieved significant results. However, there have been few studies on organ-specific tumor metastasis, including the molecular mechanism that determines the organ-specific metastasis of GC. GC metastasis clinical specimens are difficult to obtain; therefore, there is a lack of an effective cell model for GC with high metastatic potential[6-7]. This study analyzed the expression of Ki-67 and microRNA-27a (miR-27a) in the lesion tissues of patients with early-stage GC and their depth of infiltration to deepen the understanding of the prediction and prognosis of GC metastasis and provide a reliable genetic level for the screening and diagnosis of high-risk groups. The common detection index improves the early diagnosis rate of GC, predicts metastasis and

prognosis, and provides more theoretical support for treatment[8-9]. The expression of Ki-67 reflects the degree of cell proliferation and is related to the biological behavior of GC. Mohamedi et al. believed that fibrin not only acts as a molecular bridge within the cell microenvironment but also affects cell behavior[10-11]. Fibulin-5 has been shown to promote and protect tumors through a mechanism that is not fully understood[12-13].

The basis of these anti-tumor effects is the reduction of phosphorylation levels of Ser residues involved in β-catenin nuclear translocation[14-15]. A decrease in Fibulin-5 expression corresponds to an increase in Ki-67 detection in breast tissue samples[16-17]. While this research is theoretically correct, it lacks data verification. Detection of miR-27a in peripheral blood circulation has shown that it is significantly up-regulated in GC patients. MiR-27a can be used as an early non-invasive diagnostic method and is a good indicator of prognosis. Cui et al. found that miR-27a-3p levels were up-regulated in transforming growth factor-β1 treated human lung fibroblasts in a Smad2/3-dependent manner[18] and in the lungs from mice with experimental lung fibrosis. Isolated fibroblasts were up-regulated[19-20]. However, compared with the control group, miR-27a-3p expression induced by basal and transforming growth factor β1 was reduced[21-22].

When a particle is reduced to a nanometer size, it develops new acoustic, optical, electrical, magnetic, and thermal properties. For example, the widely studied II-VI group semiconductor cadmium sulfide, the position of the absorption band boundary, and the peak position of the emission spectrum are significantly blue-shifted as the grain size decreases. According to this principle, cadmium sulfide with different energy gaps can be obtained by controlling the grain size, which will greatly enrich the research content of materials and enable new uses. However, the types of substances are limited. Both micron and nanometer cadmium sulfides are composed of sulfur and cadmium; however, by controlling the preparation conditions, materials with different band gaps and luminescence properties can be obtained.

Therefore, new materials are obtained through nanotechnology. Nanoparticles often have a large specific surface area. The specific surface area per gram can reach hundreds or even thousands of square meters, which makes them useful as highly active adsorbents and catalysts in hydrogen storage, organic synthesis, and environmental protection. Other fields have important application prospects. "lighter, taller, and stronger" can be used to summarize nanoparticles. "Lighter" means that with the help of nanomaterials and technology, we can prepare devices with smaller sizes, unchanged or better performance, and lighter weights. For example, the first computer needed three houses to store it. Micron-level semiconductor manufacturing technology helped miniaturize this, and computers were popularized. Regardless of the energy and resource utilization, the benefits of this miniaturization are significant. "Higher" means that nanomaterials are expected to have higher optical, electrical, magnetic, and thermal properties. "Strong" means that nanomaterials have stronger mechanical properties, such as strength and toughness. Regarding nanoceramics, nanocrystallization is expected to solve the brittleness problem of ceramics and may exhibit similar plasticity to metals and other materials. This study assessed the expression and infiltration depth of Ki-67 and MiR-27ain in early-stage GC patients. In addition, we studied the invasion and metastasis mechanisms of GC, searched for new diagnostic markers, provided a theoretical basis for studying the occurrence, development, and prognosis of GC, and provided a basis for new clinical treatment targets.

Materials and methods

Research object

Fifty clinically diagnosed GC specimens were collected from patients who were not treated with radiotherapy or chemotherapy before surgery. The specimens were collected from 38 males and 12 females. The age range of patients was 37-75 years old, including 12 cases <50 years old and 38 cases ≥50 years old; the average age was 56 years old. The control group consisted of 20 normal gastric mucosa tissues collected 5 cm away from the tumor edge.

Main reagents

The main reagents used were ki67Antibody-Biotin, trypsin, ZymoTaqPreMix, related primer synthesis, DEPC, TRIzol reagent, Taq Master Mix, fetal bovine serum (FBS), Trans DNA MarkerI, miR27a antagomir, and xylene[23].

Main instruments

The main instruments used were a paraffin slicer, automatic constant temperature spreadsheet baking machine, electric heating constant temperature drying oven, high-pressure steam cooker, and horizontal electrophoresis tank[24-25].

Specimen collection and processing

Material selection standard

The GC tissue samples were taken from the center of each tumor.

The sampling sites of the surrounding GC tissue of GC were relatively normal gastric mucosa that was more than 5 cm away from the outer edge of the tumor body. Collected samples were no larger than 2 × 1.5 × 0.3cm.

Specimen processing

Sealing wax for GC specimen

• Fixation: stomach cancer tissues were surgically removed and placed in 10% formalin solution for 12 hours.

• Transparent: the samples were placed in xylene I for 1 hour, then xylene II for 2 hours.

• Wax immersion: Samples were placed in mixed wax for 3 hours and pure wax for 3 hours to make a wax block.

Slicing

The LEICARM 245 microtome was used to cut pieces of GC tissue wax into uniform slices with a thickness of 4-5 μm.

Following this, samples were placed in a bleaching temperature controller, let stand, and then placed in a 65°C oven.

Experimental procedure

MiRNA extraction

• The paraffin-embedded samples of numbered pathological tissues were cut into 7um thick slices. We selected 8 pathological tissue slices and quickly placed them into corresponding 1.5 mL RNase-free centrifuge tubes. Any slices that were initially exposed to the air were discarded[26-27]. Following this, we added 1 mL of xylene to the centrifuge tubes, which were centrifuged at 12000 rpm for 10 seconds at room temperature and centrifuged for 2 minutes.

• The tubes were opened and left at room temperature or 37°C for 10 minutes.

• Lysate RF150ul and ProteinaseK10ul were added to the tubes, which were vortexed and mixed thoroughly.

• Tubes were incubated at 55°C for 15 minutes and at 80°C for an additional 15 minutes.

• The resulting RNA solutions were stored at –80°C or used for subsequent experiments.

Immunohistochemical staining

• Glass treatment: glass plates were soaked in detergent and rinsed with tap water before being dried. Plates were then soaked in a sulfuric acid cleaning solution for 24 hours and then rinsed with tap water 20 times and with distilled water 4 times. The plates were then dried in the oven. Prior to preparation, plates were coated with 10% polylysine and dried[28-29].

• Dewaxing and hydration: samples were placed in xylene 1 for 10 minutes, xylene II for 10 minutes, absolute ethanol I for 5 minutes, anhydrous ethanol II for 5 minutes, 95% ethanol for 5 minutes, 80% ethanol for 5 minutes, 5 50% ethanol for 10 minutes, and tap water for 10 minutes.

• DAB solution color development: samples were soaked in PBS solution 3 times for approximately 3 minutes each time. The appropriate proportion of DAB color developer was added dropwise, and color development was observed under a microscope. The color development time is approximately 3–5 minutes. If brown particles appeared, we rinsed the sample immediately with water to develop color.

• The samples were stained multiple times with Sugi Nouki staining solution. Excess was washed off, and samples were then placed in ordinary gradient alcohol for dehydration. Samples were sealed with neutral juice. Changes were observed under a microscope.

Statistical processing

Cells with brown particles in their nuclei were positive for Ki-67. Staining results were determined by combining staining intensity with the percentage of positive cells and performing semi-quantitative analyses. The relative expression of GC tissue was corrected by the difference in ΔCT values between miR-27a and U 6 in the 5 cm tissue taken from around each tumor. Statistical analyses were performed using SPSS 19.0 and Graphd Prism 5.0 software.

The measurement data were normally distributed and are expressed as mean ± standard deviation. T-tests were used for comparisons between two groups, while a one-way ANOVA was used for comparisons between multiple groups. The test level was set as α=0.05.

Results

Expression of Ki-67 in GC

Table 1 shows the expression of Ki-67 in normal and GC tissues. Ki-67 positive signals in

normal gastric tissue were primarily expressed in the nucleus. In the 10 normal gastric tissue specimens, 5 were negative for Ki-67 expression, 4 were weakly positive, 1 was moderately positive, and 0 were strongly positive. In the 80 GC tissue samples, 24 were negative for Ki-67 expression, 12 were weakly positive, 18 were moderately positive, and 26 were strongly positive. Among these, there were 35 samples that demonstrated high differentiation, and 45 cases demonstrated poor differentiation. Furthermore, 30 samples involved lymph node metastasis, while 50 cases involved non-lymph node metastasis. Regarding the highly differentiated samples, 16 samples were negative for Ki-67 expression, 9 were weakly positive, 6 were moderately positive, and 4 were strongly positive.

Of the fourteen samples that demonstrated lymph node metastasis, 12 were negative for Ki-67 expression, 5 were weakly positive, 7 were moderately positive, and 6 were strongly positive. Of the samples that demonstrated non-lymph node metastasis, 11 were moderate positively for Ki-67 expression, and 20 were strongly positive.

Group	N	Grade				P
		-	+	++	+++	
Normal	10	5	4	1	0	P<0.05
Gastric carcinoma differentiation	80	24	12	18	26	
Well and moderately differentiated	35	16	9	6	4	P<0.05
Poorly differentiated	45	8	3	12	22	
Lymph node metastasis	30	12	5	7	6	P<0.05
Non-lymph node metastasis	50	12	7	11	20	

Table 1: Ki-67 expression in normal and gastric cancer tissues.

Relationship between Mir-27a expression level and clinical characteristics

The relationship between the clinical features of GC pathology and miR-27a expression levels is shown in Figure 1. Age, sex, and tumor differentiation at diagnosis were not related to the expression of miR-27a, as the correlations between these were not statistically significant.

The results of the effect of miR-27a precursor transfection on miR-27a expressions are shown in Figure 2. Compared with the transfection control, miR-27a expression was significantly up-regulated 24 hours after transfection of miR-27a precursor molecules, confirming that transient transfection of miRNA-specific precursor molecules can effectively up-regulate the expression of miRNA in cells.

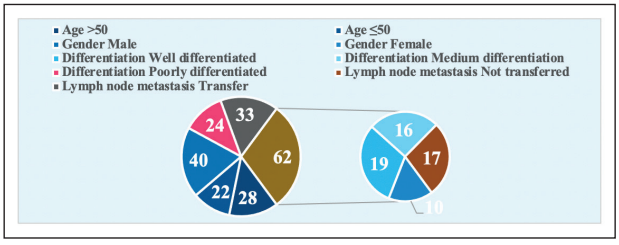

Figure 1: The relationship between the pathological clinical features of gastric cancer and miR-27a expression levels.

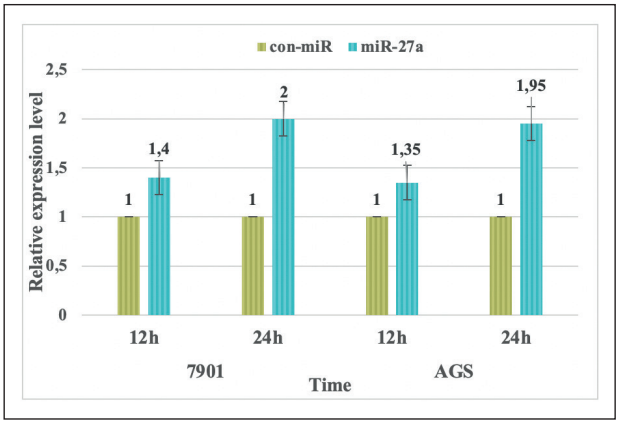

Figure 2: The effect of transfection with miR-27a-specific precursors on miR-27a expression level.

Relationship between Ki-67 expression and GC

The expression levels of Ki-67 in GC tissues are shown in Figure 3. Chronic atrophic gastritis is characterized by mucosa-specific gland atrophy and is always accompanied by intestinal epithelialization. Due to intestinal epithelialization, cells appear atypical and are prone to tumors. Ki-67 is a cell proliferation antigen whose positive expression covers the entire cell cycle.

The positive rate of Ki-67 in chronic atrophic gastritis is 73.33%, while in GC, it is 95%. The strength of Ki-67 increases with cancer and cell proliferation activity. Its expression occurs during the formation of intestinal epithelium and peaks during tumor formation. The lower the degree of cancer cell differentiation, the stronger the expression of Ki-67. Ki-67 is strongly expressed in GC patients with lymph node metastasis.

Infiltration depth analysis of Ki-67 in GC cells

The infiltration depth of Ki-67 in GC cells is shown in Figure 4. The Ki-67 antigen is a typical cell cycle-related nucleoprotein expressed in the G1, S, G2, and M phases of the cell proliferation cycle. Ki-67 expression disappears after mitosis, which is related to cellular anabolism. Its expression level

can objectively reflect tumor cells' growth state. The lower the degree of differentiation of malignant tumor cells, the slower the clinical lysis.

Therefore, the worse the degree of differentiation, the more lymph node metastasis, and the faster the cell proliferation, meaning the number of Ki-67 positive cells increase, as does its expression intensity.

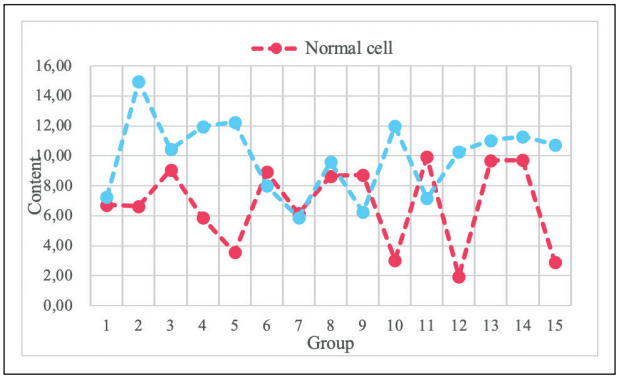

Figure 3: Ki-67 expression in gastric cancer.

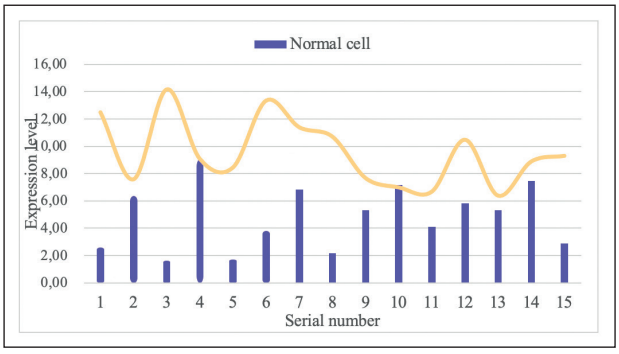

Figure 4: Ki-67 infiltration depth in gastric cancer cells.

Discussion

GC has characteristics of diffuse infiltrative growth, which can easily cause local spread and metastasis. Peritoneal metastasis is one of the most common forms of late metastasis. When single cells or small cell clusters of GC infiltrate the gastric serosa, the adhesion between gastric serous epithelial cells decreases. Tumor cells produce enzymes to dissolve the extracellular matrix, causing it to degrade and easily form defects. Tumor cells can then easily reach the peritoneum through these defects to form new metastases.

This article comprehensively studied the expression of Ki-67 and miR-27a and their depth of infiltration in the lesion tissues of patients with early-stage GC. Activation of the Wnt signaling pathway promotes cell proliferation and prevents differentiation. Regarding the use of nanomaterials, their application prospects are broad, including nanoelectronic devices, medicine and health, aerospace, aviation and space exploration, environment, resources and energy, and biotechnology. DNA has a double helix structure, and the diameter is tens of nanometers. Using synthetic light-emitting semiconductor grains with a grain size of only a few nanometers, selectively adsorbing or acting on different base pairs can "illuminate" the structure of DNA, similar to a pagoda full of lanterns in the dark. With the help of luminous "lanterns," we can recognize not only the appearance of the lighthouse but also its structure. In short, these nanocrystals are labeled with DNA molecules. At present, we should avoid the vulgarization of nanomaterials. Although scientists have been studying the application of nanomaterials and technologies, many of these are yet to directly benefit mankind.

Ki-67 and miR-27a demonstrated low expression of the FHIT gene. With an increase in cancer focus, degree of differentiation, depth of invasion, lymph node metastasis, and clinical division, the expression of FHIT in GC tissue gradually decreases, while the expression of Ki-67 gradually increases. MiR-27a demonstrates a malignant increase in GC, rapid growth, and an increased ability to invade and migrate.

References

1) Cuylen S, Blaukopf C, Politi AZ., 2016. Ki-67 acts as a biological surfactant to disperse mitotic chromosomes. Nature, 535(7611): 308-312.
2) Castagnaro M, De Maria R, Bozzetta E.,2016. Ki-67 as an indicator of the post-surgical prognosis in feline mammary carcinoma. Research in Veterinary Science, 65(3): 223.
3) Yunbao P, Yufen Y, Guoshi L., 2017. P53 and Ki-67 as prognostic markers in triple-negative breast cancer patients. Plos One, 12(2): e0172324-.
4) Fabbri A, Cossa M, Sonzogni A., 2017. Ki-67 labeling index of neuroendocrine tumors of the lung has a high level of correspondence between biopsy samples and surgical specimens when strict counting guidelines are applied. Virchows Archiv, 470(2): 153-164.
5) Luo Y, Zhang X, Mo M., 2016. High Ki-67 immunohistochemical reactivity correlates with poor prognosis in bladder carcinoma. Medicine, 95(15): e3337.

6) Yang F, Yu X, Bao Y., 2016. Prognostic value of Ki-67 in solid pseudopapillary tumor of the pancreas: Huashan experience and systematic review of the literature. Surgery,159(4): 1023-1031.
7) Cidado J, Wong HY, Rosen DM., 2016. Ki-67 is required for maintenance of cancer stem cells but not cell proliferation. Oncotarget, 7(5): 6281-6293.
8) Yalcin SE, Ocal I, Yalcin Y., 2017. Evaluation of the Ki-67 proliferation index and urocortin expression in women with ovarian endometriomas. Eurasian Journal of Medicine, 49(2): 107-112.
9) Ko GH, Go SI, Lee WS., 2017. Prognostic impact of Ki-67 in patients with gastric cancer—the importance of depth of invasion and histologic differentiation. Medicine, 96(25): e7181.
10) Mohamedi Y, Fontanil T, Solares L.,2016. Fibulin-5 downregulates Ki-67 and inhibits proliferation and invasion of breast cancer cells. International Journal of Oncology, 48(4): 1447-1456.
11) Peres AL, Maria PESK, de Araújo RFF., 2016. Immunocytochemical study of TOP2A and Ki-67 in cervical smears from women under routine gynecological care. Journal of Biomedical Science, 23(1): 42.
12) Saha M, Chakraborty C, Arun I., 2017. An advanced deep learning approach for Ki-67 stained hotspot detection and proliferation rate scoring for prognostic evaluation of breast cancer. Scientific Reports, 7(1): 3213.
13) Zeggai S, Harir N, Tou A., 2016. Immunohistochemistry and scoring of Ki-67 proliferative index and p53 expression in gastric B cell lymphoma from Northern African population: A pilot study. Journal of Gastrointestinal Oncology, 7(3): 462-468.
14) Lawrence NF, Hammond MR, Frederick DT., 2016. Ki-67, p53, and p16 expression, and G691S RET polymorphism in desmoplastic melanoma (DM): A clinicopathologic analysis of predictors of outcome. Journal of the American Academy of Dermatology, 75(3): 595-602.
15) Dmitrenko AP., 2016. Lateral differences in Ki-67 in breast cancer. Molecular & Clinical Oncology, 4(6): 1041-1044.
16) Mahadevappa A., 2017. Diagnostic and prognostic significance of Ki-67 immunohistochemical expression in surface epithelial ovarian carcinoma. Journal of Clinical & Diagnostic Research, 11(2): 8-12.
17) Li L, Han D, Wang X., 2017. Prognostic values of Ki-67 in neoadjuvant setting for breast cancer: A systematic review and meta-analysis. Future Oncology, 13(17): 1021-1034.
18) Cui H, Banerjee S, Xie N., 2016. MicroRNA-27a-3p is a negative regulator of lung fibrosis by targeting myofibroblast differentiation. Am J Respir Cell Mol Boil, 54(6): 843-852.
19) Wang ZH, Yang HL., 2016. EMMPRIN, SP1, and microRNA-27a mediate physcion 8–O–β–glucopyranoside - induced apoptosis in osteosarcoma cells. American Journal of Cancer Research, 6(6): 1331-1344.
20) Lv YN, Ou-Yang AJ, Fu LS., 2017. MicroRNA-27a negatively modulates the inflammatory response in lipopolysaccharide-stimulated microglia by targeting TLR4 and IRAK4. Cellular & Molecular Neurobiology, 37(2): 195-210.
21) Hou X, Tian J, Geng J., 2016. MicroRNA-27a promotes renal tubulointerstitial fibrosis by suppressing the PPARγ pathway in diabetic nephropathy. Oncotarget, 7(30): 47760-47776.
22) Ali HO, Arroyo AB, González-Conejero R.,2016. The role of microRNA-27a/b and microRNA-494 in estrogen-mediated downregulation of tissue factor pathway inhibitor α. Journal of Thrombosis & Haemostasis, 14(6): 1226-1237.
23) Shi DL, Shi GR, Xie J., 2016. MicroRNA-27a inhibits cell migration and invasion of fibroblast-like synoviocytes by targeting follistatin-like protein 1 in rheumatoid arthritis. Molecules & Cells, 39(8): 611-618.
24) Wu F, Li J, Guo N., 2017. MiRNA-27a promotes the proliferation and invasion of human gastric cancer MGC803 cells by targeting SFRP1 via Wnt/β-catenin signaling pathway. American Journal of Cancer Research, 7(3): 405-416.
25) Zeng G, Xun W, Wei K., 2016. MicroRNA-27a-3p regulates epithelial to mesenchymal transition via targeting YAP1 in oral squamous cell carcinoma cells. Oncology Reports, 36(3): 1475-1482.
26) Liu M, Khan A, Wang Z, Liu Y, Yang G, Deng Y, He N., 2019. Aptasensors for pesticide detection. Biosensors & Bioelectronics, 130: 174-184.
27) Huang RR, He L, Xia YY, Xu HP, Liu C, Xie H, Wang S, Peng LJ, Liu YF, Liu Y, He NY, Li, ZY., 2019. A sensitive aptasensor based on a hemin/G-quadruplex-assisted signal amplification strategy for electrochemical detection of gastric cancer exosomes. Small, 15(19): e1900735(1)-e1900735(7).
28) Liu Y, Li T, Ling C, Chen Z, Deng Y, He N., 2019. Electrochemical sensor for Cd2+ and Pb2+ detection based on nanoporous pseudo carbon paste electrode. Chinese Chemical Letters, 30(12): 2211-2215.
29) Yu X, He L, Pentok M, Yang H, Yang Y, Li Z, He N, Deng Y, L, S, Liu T, Chen X, Luo H., 2019. An aptamer-based new method for competitive fluorescence detection of exosomes. Nanoscale, 11(33): 15589-15595.

Corresponding Author:
Wei Mao
19 Xiuhua Road, Xiuying District, Haikou City, Hainan Province, China
Email: weimaowm@outlook.com
(China)